S. H. Chen · B. Feng

Size effect in micro-scale cantilever beam bending

Abstract When the thickness of metallic cantilever beams reduces to the order of micron, a strong size effect of mechanical behavior has been found. In order to explain the size effect in a micro-cantilever beam, the couple-stress theory (Fleck and Hutchinson, J Mech Phys Solids 41:1825–1857, 1993) and the C-W strain gradient theory (Chen and Wang, Acta Mater 48:3997–4005, 2000) are used with the help of the Bernoulli–Euler beam model. The cantilever beam is considered as the linear elastic and rigid-plastic one, respectively. Analytical results of the cantilever beam deflection under strain gradient effects by applying these two kinds of theories are obtained, from which we find an explicit relationship between the intrinsic lengths introduced in the two kinds of theories. The theoretical results are further used to analyze the experimental observations, and predictions by both theories are further compared. The results in the present paper should be useful for the design of micro-cantilever beams in MEMS and NEMS.

1 Introduction

Plenty of experiments have shown that metallic material behavior displays a strong size effect when the characteristic length scale is on the order of the micron or submicron scale. In micro-torsion tests, Fleck et al. [3] observed the presence of material hardening of thin copper wires as the wire diameter decreases from 170 to 12 μm; Micro-indentation and nano-indentation tests have shown an increasing material hardness with reducing indentation sizes [4–14]. Experiments for the particle-reinforced composites [15] have shown an obvious increase in the macroscopic flow stress through decreasing the particle diameter from 165 μm to 4.5 μm, while the volume fraction of the particle is kept constant. Moreover, with the development of MEMS and NEMS [16–18], micro-beams have been widely applied. However, the mechanical behavior of the micro-beam cannot be described directly by the classical beam bending theory, due to the existing size effect shown in many experimental observations [19–23]. Many other well-known problems also show a strong size effect, such as the increasing yield and flow stresses in polycrystalline materials with decreasing grain diameter [24,25] or the increasing fracture toughness in the micron regions ahead of a crack tip [26].

The classical elasto-plasticity theories with the absence of an intrinsic length scale in the constitutive relations cannot be applied to explain and predict the strong size dependence of metallic materials at micron or submicron scale. Inspired by the aforementioned size effects in experiments, a number of strain gradient theories have been proposed to address these problems through the introduction of intrinsic length scale measures in the constitutive relations, which are mostly based on the continuum mechanics concepts.

S. H. Chen (✉) · B. Feng
LNM, Institute of Mechanics, Chinese Academy of Sciences,
Beijing 100190, China
E-mail: chenshaohua72@hotmail.com
Tel.: +86-10-82543960
Fax: +86-10-82543977

There are two kinds of frameworks of strain gradient plasticity theories. The first one is typically Mindlin's framework [27,28] of higher-order continuum theories, which involves the higher-order stress as the work conjugate of the strain gradient. In these higher-order strain gradient theories, the order of the equilibrium equations is higher than that of the conventional continuum theories, so additional boundary conditions are introduced. Examples in this class include Fleck and Hutchinson [1,29,30], Fleck et al. [3], Fleck and Willis [31], Gao et al. [32,33], Gurtin [34,35], Huang et al. [36,37], Hwang et al. [38,39], Lam et al. [21], Yang et al. [40], and Yi et al. [41]. The other framework of strain gradient plasticity theories does not involve the higher-order stress and requires no additional boundary conditions. The plastic strain gradient comes into play through the incremental plastic modulus. Examples in this class include Acharya and Beaudoin [42], Chen and Wang [2], Bassani [43], Evers et al. [44], and Huang et al. [45].

The gradient concept has been extended to the gradient damage theories that have been developed for isotropic damage (e.g. Peerlings et al. [46]) and for anisotropic damage (e.g. Voyiadjis et al. [47]; Voyiadjis and Dorgan [48]). In addition, extension of the gradient theories to rate-dependent plasticity or damage has been made for few studies (e.g. Aifantis et al. [49]; Gurtin [50]; Voyiadjis et al. [51]; Wang et al. [52]).

The strain gradient plasticity theories have given reasonable agreements with the aforementioned size dependence in several typical experiments, such as thin-wire torsion (e.g. Chen and Wang [2,53,54]; Fleck et al. [3]; Gao and Huang [55]), thin-beam bending (e.g. Chen and Wang [2,53,54]; Gao and Huang [55]; Stolken and Evans [23]), micro- and nano-indentation (e.g. Chen et al. [56]; Huang et al. [37]; Nix and Gao [57]; Saha et al. [12]; Wei and Hutchinson [58]; Xue et al [59]) as well as the composite material experiments (e.g. Chen and Wang [60]; Fleck and Hutchinson [29]; Shu and Fleck [61]; Wei [62]; Liu and Hu [63]).

Although there has been tremendous theoretical work to understand the physical role of the gradient theories, this research area is still in its critical state with numerous controversies. One of them is the physical meaning of the introduced intrinsic length, whose definition and magnitude are keys to the development of the strain gradient plasticity theories. This issue has attracted many researchers' interests, among which Gao et al. [33] and Huang et al. [36] introduced the intrinsic material length into their MSG theory based on the Taylor dislocation and identified the intrinsic length as $(\mu/\sigma_Y)^2\, b$, where μ is the shear modulus, σ_Y the yield stress, and b the Burgers vector. Voyiadjis and Abu Al-Rub [64] discussed in detail the length scale parameter and proposed a physically based relationship for the length scale parameters as functions of the course of deformation and the material micro-structural features. As for the phenomenological strain gradient theories, such as Chen and Wang [2,53,54], Fleck and Hutchinson [1,29,30], and Hu et al. [65], the intrinsic length can be obtained from the calibration of experimental data. One question is that different strain gradient theories achieve different intrinsic length scales through the calibration. Are there any physical links among them? How can we obtain the intrinsic length scale for one kind of strain gradient theory from the prediction of another strain gradient theory?

One of our motivations in the present paper is to answer the above questions. We choose a micro-cantilever beam bending model in the present paper as a typical example. Both the couple-stress theory (CS) proposed by Fleck and Hutchinson [1] and the strain gradient theory (C-W) proposed by Chen and Wang [2] will be used because of their simplicity and both belonging to phenomenological ones. As for the other popular gradient theories in the literature, an analysis on the relationship of length scales among them can also be done, such as MSG and TNT theories [32,45].

The micro-beam bending problem has already been analyzed in several works using different strain gradient theories, such as Wang et al. [66], Lam et al. [21], McFarland and Colton [67], Park and Gao [68], Ma et al. [69], Challamel and Wang [70], Giannakopoulos and Stamoulis [71], Ji et al. [72], and Shi et al. [73]. Whether the simple C-W strain gradient theory [2] could predict the size effect in a micro-cantilever beam is another motivation that we present in this paper. Similar to [68], the Bernoulli–Euler beam model is adopted in the present paper. A rigid-plastic model is studied first by the simple couple-stress theory [1] and C-W strain gradient one [2] and then the elastic one. The results in this paper should be useful in the fields of MEMS and NEMS to measure precisely the mechanical behavior of micro-cantilever beams.

2 Brief summary of strain gradient theory

2.1 The couple-stress theory

Based on the generalized classical J_2 deformation theory and higher-order continuum theory (Mindlin [27,28]; Mindlin and Tiersten [74]; Toupin [75]), the well-known couple-stress theory was proposed by Fleck and Hutchinson [1]. They assumed that the strain energy density of a homogeneous isotropic solid depends upon

the scalar invariants of the strain tensor ε and the curvature tensor χ through a generalized effective strain E_e. An overall stress measure Σ_e is defined as the work conjugate of E_e and is an unique function of the overall strain measure E_e. The virtual work done on the solid per unit volume equals the increment in strain energy density,

$$\delta\omega = \Sigma_e \delta E_e + \sigma_m \delta\varepsilon_m = \sigma' : \delta\varepsilon' + m^T : \delta\chi + \sigma_m \delta\varepsilon_m, \tag{1}$$

where

$$E_e^2 = \varepsilon_e^2 + l_{cs}^2 \chi_e^2, \quad \varepsilon_e^2 = \frac{2}{3}\varepsilon'_{ij}\varepsilon'_{ij}, \tag{2}$$

$$\varepsilon'_{ij} = \varepsilon_{ij} - \frac{1}{3}\varepsilon_m \delta_{ij}, \quad \varepsilon_{ij} = \frac{1}{2}(u_{i,j} + u_{j,i}) \qquad \varepsilon_m = \varepsilon_{kk} \tag{3}$$

and the curvature tensor and rotation vector are defined as

$$\chi_e^2 = \frac{2}{3}\chi_{ij}\chi_{ij}, \quad \chi_{ij} = \theta_{i,j}, \quad \theta_i = \frac{1}{2}e_{ijk}u_{k,j}. \tag{4}$$

Then, the deviatoric stress tensor σ', couple-stress tensor m and σ_m can be obtained as

$$\sigma'_{ij} = \frac{\partial\omega}{\partial\varepsilon'_{ij}} = \frac{2}{3}\frac{\Sigma_e}{E_e}\varepsilon'_{ij}, \tag{5}$$

$$m_{ij} = \frac{\partial\omega}{\partial\chi_{ji}} = \frac{2}{3}\frac{\Sigma_e}{E_e}l_{cs}^2\chi_{ji}, \tag{6}$$

$$\sigma_m = \frac{\partial\omega}{\partial\varepsilon_m} \tag{7}$$

where

$$\Sigma_e = (\sigma_e^2 + l_{cs}^{-2}m_e^2)^{1/2}, \tag{8}$$

$$\sigma_e^2 = \frac{3}{2}\sigma'_{ij}\sigma'_{ij}, \quad m_e^2 = \frac{3}{2}m_{ij}m_{ij}, \quad \sigma_m = \frac{\sigma_{kk}}{3}. \tag{9}$$

2.2 The C-W gradient theory

Inspired by Acharya and Bassani [76], in which they conclude that the only possible formulation is a flow theory with strain gradient effects represented as an internal variable to increase the current tangential-hardening modulus, Chen and Wang proposed a C-W strain gradient theory [2], in which it preserves the essential structure of the incremental version of conventional J_2 deformation theory. No higher-order stresses or higher-order strain rates are introduced so that no extra boundary value conditions beyond the conventional ones are required in the strain gradient theory.

In the conventional plasticity theories, σ_e is the work conjugate of ε_e and defined by

$$\sigma_e = \frac{d\omega(\varepsilon_e)}{d\varepsilon_e}, \quad \sigma_e = \sqrt{\frac{3}{2}\sigma'_{ij}\sigma'_{ij}}. \tag{10}$$

The work done per unit volume equals the increment in strain energy density

$$\delta\omega = \sigma' : \delta\varepsilon' + \sigma_m : \delta\varepsilon_m \tag{11}$$

where the deviatoric stress tensor σ'_{ij} can be obtained as

$$\sigma'_{ij} = \frac{\partial\omega}{\partial\varepsilon'_{ij}} = \frac{2}{3}\frac{\sigma_e}{\varepsilon_e}\varepsilon'_{ij}. \tag{12}$$

then, the incremental form can be expressed as

$$\sigma'_{ij} = \frac{2}{3}\frac{\varepsilon'_{ij}}{\varepsilon_e}\dot{\sigma}_e + \frac{2}{3}\frac{\dot{\varepsilon}'_{ij}}{\varepsilon_e}\dot{\sigma}_e - \frac{2}{3}\frac{\varepsilon'_{ij}\sigma_e}{\varepsilon_e^2}\dot{\varepsilon}_e. \tag{13}$$

The incremental form of the classical hardening relationship can be expressed as

$$\dot{\sigma}_e = A'(\varepsilon_e)\dot{\varepsilon}_e. \tag{14}$$

In order to consider the effect of strain gradient, a new incremental hardening law is introduced,

$$\dot{\sigma}_e = A'(\varepsilon_e)\left(1 + \frac{l_{cw}\eta}{\varepsilon_e}\right)^{1/2}\dot{\varepsilon}_e = B(\varepsilon_e, l_{cw}\eta)\dot{\varepsilon}_e \tag{15}$$

where η is defined as

$$\eta = \sqrt{c_1\eta^{(1)}_{ijk}\eta^{(1)}_{ijk} + \chi_e^2}. \tag{16}$$

$\eta^{(1)}_{ijk}$ is defined as the stretch gradient [29] and $c_1 = \left(\frac{l_1}{l_{cw}}\right)^2$. Here, l_1 and l_{cw} are defined as intrinsic length scales for the stretch and rotation gradients, respectively.

One can see that the C-W strain gradient model belongs to the second class (simple theory) mentioned in the Introduction that does not include any higher-order stress or extra boundary condition.

Recently, there is another controversy raised by Acharya and Bassani [76,77], Acharya et al. [78] and Volokh and Hutchinson [79], that is whether the simple strain gradient theories in the framework proposed by Acharya and Bassani [76] are physically admissible. As part of the analysis of a particular problem (simple shearing), the latter researchers question the physical validity of the nature of boundary conditions that they designate as applicable to the model. Furthermore, with the simple theory for a particular choice of hardening law, Niordson and Hutchinson [80] demonstrate numerically the phenomenon of "vertex localization" with a trend toward localization of high strain in a narrow band, in small-deformation hardening plasticity. Niordson and Hutchinson [80] suggest that such a phenomenon is to be expected as a general feature of the simple theory due to the nature of its mathematical formulation and regardless of the specific choice of hardening description employed. However, Acharya et al. [78], through linearized analysis and computation, show that lower-order gradient plasticity is compatible with boundary conditions. A physically motivated gradient modification of the conventional hardening law can lead to a convective stabilizing effect in 1-D, rate-independent plasticity. The partial differential equation is genuinely non-linear and does not arise as a conservation law. Example problems are solved numerically in Acharya et al. [78], which show the robustness and simplicity of physically motivated lower-order gradient plasticity.

On the other hand, whether the strain gradient plasticity theories are compatible with thermodynamics is discussed by Gurtin and Anand [81], in which a general discussion of the virtual-power principle applied to small-deformation theories of plasticity is begun with and the physical nature of flow rules for rate-independent gradient plasticity theories are discussed. Finally, they found that the flow rule of Fleck and Hutchinson [30] is incompatible with thermodynamics unless its non-local term is dropped. If the underlying theory is augmented by a general defect energy dependent on the plastic strain γ^p and $\nabla\gamma^p$, then compatibility with thermodynamics requires that its flow rule reduces to that of Aifantis [82]. Recently, Kuroda and Tvergaard [83] developed a phenomenological higher-order strain gradient plasticity theory, in which all the development has been expressed by the conventional stress quantities and the origin of the gradient term is interpreted in terms of dislocation theory. By contrast, in the study by Gurtin and Anand [81], one may derive specific constitutive equations formally in a thermodynamically consistent manner, and this procedure is totally based on the extended virtual work principle, which emphasizes the existence of higher-order stresses and higher-order tractions. Whether the simple strain gradient theory (the lower-order strain gradient plasticity theories including the present C-W model) is compatible with thermodynamics as the higher-order gradient theories (e.g., Kuroda and Tvergaard [83]; Mühlhaus and Aifantis [84]; Abu Al-Rub et al. [85]) should be checked in the future work.

3 The solution of basic quantities for cantilever beam bending

Similar to Park and Gao [68], a Bernoulli–Euler cantilever beam model is adopted in the present paper as shown in Fig. 1, in which the mid-plane is set as the $x - y$ plane of a Cartesian coordinate system (x, y, z), the y-axis is along the width direction and the z-axis is along the direction of beam thickness. The total length of the cantilever beam is L. The displacement functions for the cantilever beam can be expressed as (see Reddy [86])

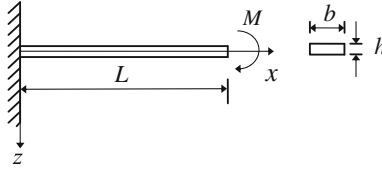$$u_1 = [u_1(x)]_s - zw'(x), \quad u_2 = 0, \quad u_3 = w(x) \tag{17}$$

Fig. 1 A micro-cantilever beam with an applied moment M at the free end. L is the beam length, b the width, and h the thickness

where the subscript s refers to the quantity induced by the axial stretching. In the present paper, all derivations are based on a vanishing axial stretching action, i.e. $[u_1(x)]_s = 0$.

Thus, the strain components can be obtained as

$$\varepsilon_{xx} = -zw''(x), \tag{18}$$

$$\varepsilon_{yy} = \varepsilon_{zz} = \varepsilon_{xy} = \varepsilon_{yz} = \varepsilon_{zx} = 0 \tag{19}$$

which yield the volumetric strain, non-vanishing deviatoric strain, and the effective strain

$$\varepsilon_m = -zw''(x), \quad \varepsilon'_{xx} = -\frac{1}{2}\varepsilon'_{yy} = -\frac{1}{2}\varepsilon'_{zz} = -\frac{2}{3}zw''(x), \quad \varepsilon_e = \frac{2}{3}\left|zw''(x)\right|. \tag{20}$$

The non-vanishing rotation components and curvatures can be written as

$$\theta_y = -w'(x), \quad \chi_{yx} = -\frac{d^2w(x)}{dx^2} = -w''(x) \tag{21}$$

which results in the effective rotation gradient,

$$\chi_e^2 = \frac{2}{3}w''^2. \tag{22}$$

Due to the ultra-thin thickness of the cantilever beam, it is reasonable to assume

$$\sigma_{zz} = 0. \tag{23}$$

Then, the linear elastic relation between the effective stress and effective strain can be written as

$$\sigma_e = \frac{3E}{2(1+v)}\varepsilon_e \tag{24}$$

where E is Young's modulus and v is the Poisson ratio.

According to Shame and Dym [87], the displacement functions for a Bernoulli–Euler beam require $v = 0$, which leads to

$$\sigma_e = \frac{3}{2}E\varepsilon_e. \tag{25}$$

For a rigid-plastic linear-hardening solid, we can easily obtain

$$\sigma_e = \Sigma_0 + \frac{3}{2}E_p\varepsilon_e \tag{26}$$

where Σ_0 and E_p denote the yield strength and hardening modulus respectively.

In the present paper, the Bernoulli–Euler beam is assumed to be rigid-plastic, not elastic-plastic for two reasons. The first one is for simplicity and analytical solutions can be found using the strain gradient theories though beams of linearly elastic-strain hardening plastic materials undergoing large deformations have been solved by Zhu [88] using the classical theory. The second one is for consistency with the existing experimental observations (Stolken and Evans [23]), in which beam bending with thickness in micrometers exhibits almost a rigid-plastic behavior.
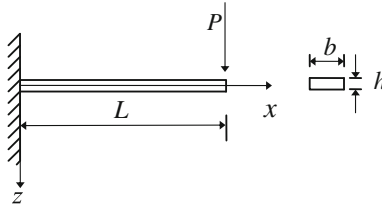
Fig. 2 A cantilever beam with an applied concentrated force P at the free end

4 Size effect predicted by the couple-stress theory

The couple-stress theory proposed by Fleck and Hutchinson [1] will be used in this Section to analyze the size effect in micro-cantilever beam bending. Two kinds of loading forms will be considered, respectively. One is a bending moment as shown in Fig. 1, and the other is a concentrated force added at the end of the cantilever beam as shown in Fig. 2. The deflection of the beam with the strain gradient effect will be focused.

4.1 Cantilever beam bending subject to a moment at the free end

4.1.1 The case of a rigid-plastic linear-hardening beam

Consider the case of a micro-cantilever beam subject to a moment M at the end. According to the couple-stress theory (CS) [1], the rigid-plastic linear-hardening relation can be obtained by substituting σ_e and ε_e in Eq. (26) with Σ_e and E_e, respectively,

$$\Sigma_e = \Sigma_0 + \frac{3}{2} E_p E_e, \tag{27}$$

where Σ_e and E_e are the generalized effective stress and the generalized effective strain defined in Eqs. (8) and (2), respectively.

The non-vanishing deviatoric stress components and couple stresses can be obtained from Eqs. (5), (6) and (20) as

$$\sigma'_{xx} = \frac{2}{3} \frac{\Sigma_e}{E_e} \varepsilon'_{xx}, \quad \sigma'_{yy} = \sigma'_{zz} = -\frac{1}{3} \frac{\Sigma_e}{E_e} \varepsilon'_{xx}, \quad m_{xy} = \frac{2}{3} \frac{\Sigma_e}{E_e} l_{cs}^2 \chi_{yx}. \tag{28}$$

The bulk stress can be written as

$$\sigma_m = -\sigma'_{zz} = \frac{\sigma'_{xx}}{2}, \tag{29}$$

then

$$\sigma_{xx} = \frac{2}{3} \frac{\Sigma_e}{E_e} \varepsilon_{xx}. \tag{30}$$

Assuming the applied moment M is large enough to render the overall beam deformed, the strain energy is given by

$$U = \int_V \omega dv. \tag{31}$$

Using the principle of minimum total potential energy yields

$$\delta\pi = \int_V \delta\omega dv - M\delta w'(L)$$

$$= (k_2 w'' + k_1)\delta w'\big|_0^L - k_2 w'''\delta w\big|_0^L + \int_0^L k_2 w^{(4)}\delta w dx - M\delta w'(L) = 0 \tag{32}$$

where k_1 and k_2 are two constants related to the intrinsic length l_{FP},

$$k_1 = \frac{\Sigma_0 bh}{4}\sqrt{h^2 + 6l_{FP}^2} + \frac{\Sigma_0 bl_{FP}^2}{2}\ln\left(\sqrt{\frac{h^2}{6l_{FP}^2} + 1} + \frac{\sqrt{6}}{6}\frac{h}{l_{FP}}\right),$$

$$k_2 = bE_p h\left(\frac{h^2}{12} + l_{FP}^2\right). \tag{33}$$

Here, l_{FP} represents the intrinsic length l_{cs} in CS theory [1] for a rigid-plastic case.

The boundary conditions at the fixed end, i.e., $x = 0$, can be described as

$$w(0) = 0, \qquad w'(0) = 0, \tag{34}$$

and those at the free end $x = L$ are

$$M|_{x=L} = \int_A \left(m_{xy} + \sigma_{xx}z\right)dA\bigg|_{x=L} = -(k_2 w''(L) + k_1) = -M, \tag{35}$$

$$M'|_{x=L} = -k_2 w'''(L) = 0. \tag{36}$$

Combining Eqs. (34–36) and (32) yields the governing equation,

$$k_2 w^{(4)} = 0. \tag{37}$$

Then, the deflection of the cantilever beam can be expressed as

$$w = \frac{M - k_1}{2k_2}x^2. \tag{38}$$

From Eq. (38), one can see that the deflection is obviously influenced by the size of the cantilever beam and the intrinsic length scales.

4.1.2 The case of an elastic beam

For a linear elastic cantilever beam, we have $\Sigma_0 = 0$ and $E_P = E$ in Eq. (33), then the deflection of the linear elastic cantilever beam subject to a moment at the free end can be found from Eq. (38),

$$w = \frac{M}{2E(I + bhl_{FE}^2)}x^2 \tag{39}$$

where l_{FE} denotes the intrinsic length obtained from the elastic couple-stress theory [1]. If $l_{FE} = 0$, the deflection in Eq. (39) becomes the classical solution

$$w = \frac{M}{2EI}x^2 \tag{40}$$

where

$$I = \frac{bh^3}{12}. \tag{41}$$

4.2 Cantilever beam bending subjected to a concentrated force at the free end

4.2.1 The case of a rigid-plastic linear-hardening beam

In the case of a rigid-plastic linear-hardening micro-cantilever beam subjected to a concentrated force at the free end, part of the cantilever beam will not deform. We assume that the point separating the deformational and non-deformational parts locates at $x = l_0$. Applying the principle of the minimum total potential energy, we can obtain

$$
\delta\pi = \int_0^{l_0}\int_A \delta\omega\, dA\, dx - M_a\delta w'(l_0) - P\delta w(l_0)
$$

$$
= (k_2 w'' + k_1)\delta w'\big|_0^{l_0} - k_2 w'''\delta w\big|_0^{l_0} + \int_0^{l_0} k_2 w^{(4)}\delta w\, dx - M_a\delta w'(l_0) - P\delta w(l_0)
$$

$$
= 0 \tag{42}
$$

where k_1 and k_2 are defined in Eq. (33). The moment M_a at the cross-section $x = l_0$ is determined by equation

$$
M_a = P(L - l_0). \tag{43}
$$

The boundary conditions at the fixed end, i.e., $x = 0$, are expressed as

$$
w(0) = 0, \qquad w'(0) = 0, \tag{44}
$$

and those at the cross-section $x = l_0$ are

$$
M_x(l_0) = \int_A \left(m_{xy} + \sigma_{xx}z\right) dA\,\bigg|_{x=l_0} = -(k_2 w''(l_0) + k_1) = -M_a, \tag{45}
$$

$$
M_x'(l_0) = -k_2 w'''(l_0) = P. \tag{46}
$$

Combining Eqs. (44–46) and (42) yields the governing equation,

$$
k_2 w^{(4)} = 0. \tag{47}
$$

The deflection can be solved from the above governing equations and the boundary conditions as

$$
w = \frac{Px^2}{6k_2}(3l_0 - x) \quad x \le l_0. \tag{48}
$$

As for the value of the separating point l_0, it can be obtained through the requirement

$$
\varepsilon_{xx} = 0 \quad \text{at } x = l_0 \tag{49}
$$

which yields

$$
l_0 = \left(L - \frac{k_1}{P}\right), \quad M_a = k_1. \tag{50}
$$

Then, Eq. (48) becomes

$$
w = \frac{Px^2}{6k_2}\left[3\left(L - \frac{k_1}{P}\right) - x\right] \quad x \le L - \frac{k_1}{P}. \tag{51}
$$

The rigid displacement of the non-deformable part is

$$
w = \frac{P\left(L - k_1/P\right)^2}{6k_2}\left[3x - L + \frac{k_1}{P}\right] \quad x > L - \frac{k_1}{P}. \tag{52}
$$

4.2.2 The case of an elastic beam

Considering a linear elastic cantilever beam subjected to a concentrated force at the free end. The relation between the generalized effective stress and effective strain can be obtained by substituting $\Sigma_0 = 0$ and $E_p = E$ in Eq. (33), where E is the linear elastic Young's modulus. Thus, the corresponding deflection for the linear elastic cantilever beam can be found from Eq. (51),

$$w = \frac{Px^2}{6E(I + bhl_{FE}^2)}(3L - x). \tag{53}$$

If $l_{FE} = 0$, Eq. (53) can be reduced to the classical solution,

$$w = \frac{Px^2}{6EI}(3L - x). \tag{54}$$

5 Size effect predicted by the C-W strain gradient theory

The preceding cases are investigated in this Section, but using C-W strain gradient theory. According to the definition of $\eta_{ijk}^{(1)}$ in Fleck and Hutchinson [29], $\eta_{ijk}^{(1)}\eta_{ijk}^{(1)}$ can be obtained

$$\eta_{ijk}^{(1)}\eta_{ijk}^{(1)} = \frac{2}{5}z^2(w''')^2 + \frac{4}{15}(w'')^2. \tag{55}$$

For a linear rigid-plastic cantilever beam, the hardening relation in C-W strain gradient theory is

$$\dot{\sigma}_e = \frac{3}{2}E_p\dot{\varepsilon}_e\left(1 + \frac{l_{cw}\eta}{\varepsilon_e}\right)^{1/2} \tag{56}$$

where

$$\eta = \sqrt{c_1\eta_{ijk}^{(1)}\eta_{ijk}^{(1)} + \chi_e^2} = \sqrt{c_1\left[\frac{2}{5}z^2(w''')^2 + \frac{4}{15}(w'')^2\right] + \frac{2}{3}(w'')^2}. \tag{57}$$

Since the intrinsic length corresponding to the stretch gradient l_1 is much less than that of the rotation gradient l_{cw} [23], $c_1 = (l_1/l_{cw})^2$ should be very small. From the previous study, we find that $\eta_{ijk}^{(1)}\eta_{ijk}^{(1)}$ has the same order with χ_e^2 for the ultra-thin beam. Thus, the term $c_1\eta_{ijk}^{(1)}\eta_{ijk}^{(1)}$ in Eq. (55) is negligible. Thus, the integration of Eq. (56) yields

$$\sigma_e = (\Sigma_0 + E_p\,|z|\,w'')\left(1 + \sqrt{\frac{3}{2}\frac{l_{cw}}{|z|}}\right)^{1/2}. \tag{58}$$

From the constitutive relation (12) and Eq. (20), we have non-vanishing components of the deviatoric stress

$$\sigma_{xx}' = -\frac{1}{2}\sigma_{yy}' = -\frac{1}{2}\sigma_{zz}' = \frac{2}{3}\frac{\sigma_e}{\varepsilon_e}\varepsilon_{xx}'. \tag{59}$$

Combining Eqs. (58) and (23) yields

$$\sigma_m = -\sigma_{zz}' = \frac{\sigma_{xx}'}{2}, \tag{60}$$

$$\sigma_{xx} = \frac{2}{3}\frac{\sigma_e}{\varepsilon_e}\varepsilon_{xx}. \tag{61}$$

The increment of strain energy density is

$$\delta\omega = \sigma_{xx}\delta\varepsilon_{xx}. \tag{62}$$

5.1 Cantilever beam bending subject to a moment at the free end

5.1.1 The case of a rigid-plastic linear-hardening beam

In the same way as in Sect. 4.1.1, the deflection of a rigid-plastic linear-hardening micro-cantilever beam subjected to a moment M at the free end is

$$w = \frac{M - k_3}{2k_4} x^2 \tag{63}$$

where k_3 and k_4 are constants related to the material characteristics and structure scales,

$$k_3 = \frac{1}{8} \Sigma_0 b \left[\left(2h + \sqrt{6} l_{CP} \right) \sqrt{h^2 + l_{CP} h \sqrt{6}} - 3 l_{CP}^2 \ln \left(1 + \frac{\sqrt{6}h + \sqrt{6h^2 + 6\sqrt{6} l_{CP} h}}{3 l_{CP}} \right) \right],$$

$$k_4 = E_P b \left[\frac{1}{48} \sqrt{h^2 + \sqrt{6} l_{CP} h} \left(4h^2 + \sqrt{6} l_{CP} h - 9 l_{CP}^2 \right) + \frac{3\sqrt{6}}{32} l_{CP}^3 \ln \left(1 + \frac{\sqrt{6}h + \sqrt{6h^2 + 6\sqrt{6} l_{CP} h}}{3 l_{CP}} \right) \right]. \tag{64}$$

l_{CP} represents the intrinsic length l_{cw} in the C-W strain gradient theory for a rigid-plastic case. Specifically, if $l_{CP} = 0$, k_3 and k_4 will be reduced to the classical solutions,

$$k_3 = \frac{\Sigma_0 b h^2}{4}, \quad k_4 = \frac{b E_p h^3}{12} \tag{65}$$

5.1.2 The case of a linear elastic beam

The solution to the deflection of a linear elastic beam subjected to a moment at the free end can be obtained in the same way as that in Sect. 4.1.2,

$$w = \frac{Mx^2}{Eb} \left[\frac{1}{24} \sqrt{h^2 + \sqrt{6} l_{CE} h} \left(4h^2 + \sqrt{6} l_{CE} h - 9 l_{CE}^2 \right) + \frac{3\sqrt{6}}{16} l_{CE}^3 \ln \left(1 + \frac{\sqrt{6}h + \sqrt{6h^2 + 6\sqrt{6} l_{CE} h}}{3 l_{CE}} \right) \right]^{-1}. \tag{66}$$

5.2 Cantilever beam bending subject to a concentrated force at the free end

A) Identically, we can find the deflection of a linear rigid-plastic cantilever beam subject to a concentrated force at the free end,

$$w = \frac{Px^2}{6k_4} (3l_0 - x) \quad x \le l_0 \tag{67}$$

where l_0 is the separating point between the deformable and non-deformable parts,

$$l_0 = \left(L - \frac{k_3}{P} \right). \tag{68}$$

B) The corresponding deflection of a linear elastic cantilever beam subject to a concentrated force at the free end is

$$w = \frac{Px^2(3L - x)}{3Eb \left[\frac{1}{24} \sqrt{h^2 + \sqrt{6} l_{CE} h} \left(4h^2 + \sqrt{6} l_{CE} h - 9 l_{CE}^2 \right) + \frac{3\sqrt{6}}{16} l_{CE}^3 \ln \left(1 + \frac{\sqrt{6}h + \sqrt{6h^2 + 6\sqrt{6} l_{CE} h}}{3 l_{CE}} \right) \right]} \tag{69}$$

where l_{CE} represents the intrinsic length l_{cw} in the C-W strain gradient theory for a linear elastic case.
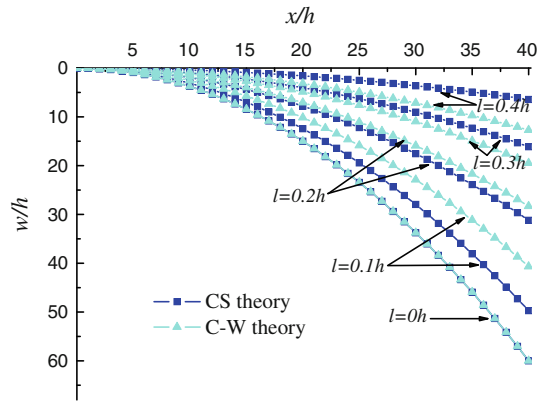
Fig. 3 The dimensionless deflection w/h along the dimensionless beam length x/h for a rigid-plastic linear-hardening micro-cantilever beam with an applied moment at the free end for different beam thicknesses, in which $L/h = 40$, $b/h = 6$, $E_P/\Sigma_0 = 40$, and $M/(\Sigma_0 bh^2) = 1/2$
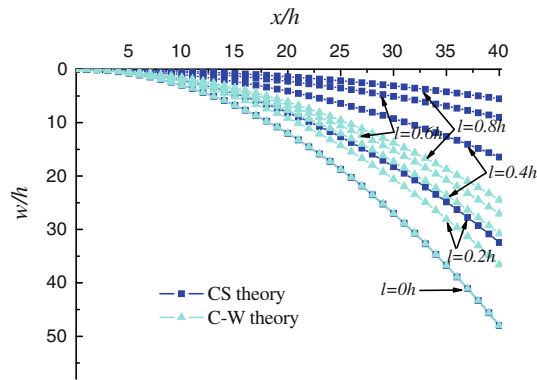

Fig. 4 The dimensionless deflection w/h along the dimensionless beam length x/h for a linear elastic micro-cantilever beam with an applied moment at the free end for different beam thicknesses, in which $L/h = 40$, $b/h = 6$, and $M/(Ebh^2) = 1/200$

6 Discussions of the theoretical predictions

6.1 Size effect of cantilever beam bending

Figures 3, 4, 5, and 6 plot the deflection of a cantilever beam as a function of the beam length for two kinds of material characteristics and two kinds of loading forms, in which we keep the intrinsic length unchanged and vary the beam's thickness. The classical solution that corresponds to a vanishing intrinsic length is also included for comparison. From Figs. 3, 4, 5 and 6, one can find the obvious size effects when the beam's thickness decreases. The bending stiffness increases along with decreasing beam's thickness, which results in a reduced deflection at a fixed point on the beam. Comparing the deflections obtained by the couple-stress and C-W strain gradient theories, one can see that for a cantilever beam: (i) predictions of both strain gradient theories can be reduced to that of the classical one; (ii) with the identical intrinsic length scale, the size effect predicted by the C-W theory is more obvious than that predicted by the couple-stress theory for a thick micro-beam; (iii) an opposite phenomenon will be found for the case of a thin micro-beam.

6.2 Relationship between the intrinsic lengths in two kinds of gradient theories

Both the couple-stress theory and the C-W strain gradient theory belong to phenomenological ones. The intrinsic length is introduced due to the requirement of the dimension. From the above, one can see that both theories can predict the size effect in the beam bending problem. Can we find the length scale in one theory
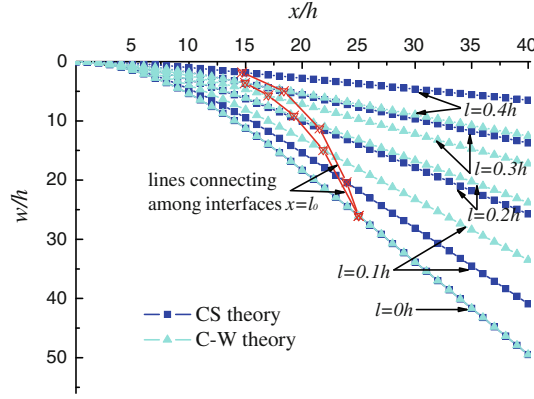
Fig. 5 The dimensionless deflection w/h along the dimensionless beam length x/h for a rigid-plastic linear-hardening micro-cantilever beam with an applied concentrated force at the free end for different beam thicknesses, in which $L/h = 40$, $b/h = 6$, $E_P/\Sigma_0 = 40$, and $PL/(\Sigma_0 bh^2) = 2/3$
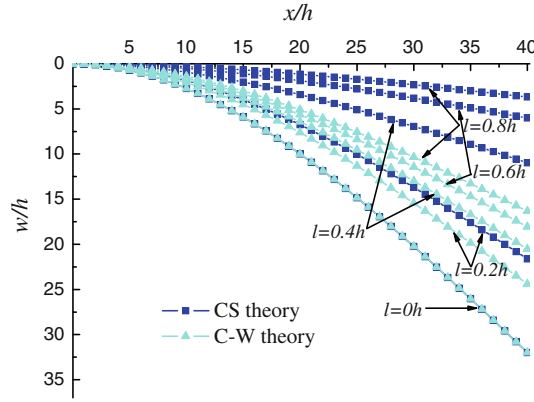

Fig. 6 The dimensionless deflection w/h along the dimensionless beam length x/h for a linear elastic micro-cantilever beam with an applied concentrated force at the free end for different beam thicknesses, in which $L/h = 40$, $b/h = 6$, and $PL/(Ebh^2) = 1/200$

from another? In the case of the linear elastic micro-cantilever beam bending, the solution of the deflection of the micro-cantilever beam bending is obtained analytically. Letting the deflections predicted by the two theories to be identical yields

$$h\left(\frac{h^2}{12} + l_{FE}^2\right) = \frac{1}{48}\sqrt{h^2 + \sqrt{6}l_{CE}h}\left(4h^2 + \sqrt{6}l_{CE}h - 9l_{CE}^2\right)$$
$$+ \frac{3\sqrt{6}}{32}l_{CE}^3 \ln\left(1 + \frac{\sqrt{6}h + \sqrt{6h^2 + 6\sqrt{6}l_{CE}h}}{3l_{CE}}\right). \quad (70)$$

The dimensionless relation between l_{FE}/h and l_{CE}/h can be obtained as

$$\left(\frac{1}{12} + \frac{l_{FE}^2}{h^2}\right) = \frac{1}{48}\sqrt{1 + \sqrt{6}\frac{l_{CE}}{h}}\left(4 + \sqrt{6}\frac{l_{CE}}{h} - 9\frac{l_{CE}^2}{h^2}\right)$$
$$+ \frac{3\sqrt{6}}{32}\frac{l_{CE}^3}{h^3} \ln\left(1 + \frac{\sqrt{6}}{3}h/l_{CE} + \sqrt{\frac{2}{3}h^2/l_{CE}^2 + \frac{2\sqrt{6}}{3}h/l_{CE}}\right) \quad (71)$$

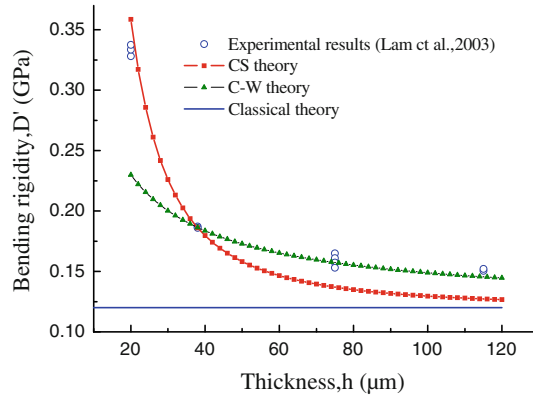where h is the thickness of the micro-cantilever beam.

Fig. 7 Comparison of bending rigidity between the theoretical results and the experimental ones (Lam et al. [21]) for a linear elastic micro-cantilever beam, in which the intrinsic length scales are $l_{CE} = 15\,\mu$m and $l_{FE} = 8.14\,\mu$m, and Young's modulus is $E = 1.44 GPa$. The bending rigidity predicted by the classical theory is also included for comparison

6.3 Comparison between the theoretical results and the experimental ones

6.3.1 Elastic case

The relation between the bending rigidity and the beam thickness is given experimentally by Lam et al. [21] for elastic micro-beams. From Eq. (39), the beam bending rigidity for the couple-stress theory can be expressed as

$$D' = \frac{E(I + bhl_{FE}^2)}{bh^3} \tag{72}$$

and that for the C-W gradient theory can be found from Eq. (66),

$$D' = Eh^{-3}\left[\frac{1}{48}\sqrt{h^2 + \sqrt{6}l_{CE}h}\left(4h^2 + \sqrt{6}l_{CE}h - 9l_{CE}^2\right) + \frac{3\sqrt{6}}{32}l_{CE}^3 \ln\left(1 + \frac{\sqrt{6}h + \sqrt{6h^2 + 6\sqrt{6}l_{CE}h}}{3l_{CE}}\right)\right]. \tag{73}$$

Both bending rigidities are consistent with the classical result $D' = E/12$ when the intrinsic length scales l_{CE} and l_{FE} vanish.

Young's modulus E of the micro-cantilever beam can be obtained to be $1.44 GPa$ from Lam et al. [21]. Using the experimental result for a typical beam thickness, e.g., $h = 38\,\mu$m, to calibrate the intrinsic length scales leads to $l_{CE} = 15\,\mu$m and $l_{FE} = 8.14\,\mu$m. Comparisons of the theoretical predictions and the experimental results are shown in Fig. 7 under the assumption that the intrinsic length keeps a constant for beams with different thicknesses, though Voyiadjis and Abu Al-Rub [64] thought the length scale parameter as a function of the course of deformation and the material micro-structural features. From Fig. 7, one can see that the theoretical predictions of the couple-stress theory are consistent well with the experimental ones for micro-beams with a relatively thin thickness, while those predicted by C-W gradient theory agree well with the experimental results for micro-beams with a relatively large thickness.

6.3.2 Rigid-plastic case

For the rigid-plastic case, the experimental results of Shrotriya et al. [22] will be compared. Using Eqs. (18), (38), and (63) yields the non-dimensional bending moment $4M/\Sigma_0 bh^2$ as a function of surface strain ε_b ($z = -h/2$).

For the CS theory, we have

$$\frac{4M}{\Sigma_0 bh^2} = 8\varepsilon_b\left(\frac{E_p}{\Sigma_0}\right)\left[\frac{1}{12} + \left(\frac{l_{FP}}{h}\right)^2\right] + \sqrt{1 + 6\left(\frac{l_{FP}}{h}\right)^2}$$
$$+ 2\left(\frac{l_{FP}}{h}\right)^2 \ln\left[\sqrt{\frac{1}{6}\left(\frac{h}{l_{FP}}\right)^2 + 1} + \frac{\sqrt{6}}{6}\left(\frac{h}{l_{FP}}\right)\right]. \tag{74}$$
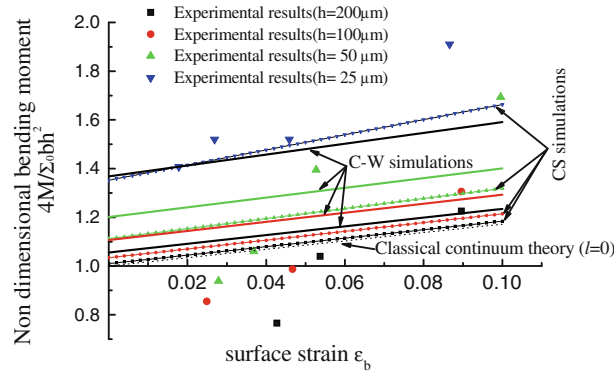
Fig. 8 Comparison of the theoretical predictions and the experimental ones (Shrotriya et al. [23]) between the non-dimensional bending moment and surface strains for a rigid-plastic linear-hardening beam, in which the intrinsic length scales are $l_{FP} = 6.5\,\mu$m and $l_{CP} = 4.8\,\mu$m, the hardening modulus is $E_P = 1.03 GPa$, yield strength $\Sigma_0 = 400\,MPa$ for $h = 25, 50, 100$, and $200\,\mu$m, respectively

For the C-W strain gradient theory, we have

$$
\frac{4M}{\Sigma_0 bh^2} = \frac{1}{6}\varepsilon_b\left(\frac{E_p}{\Sigma_0}\right)\sqrt{1+\sqrt{6}\left(\frac{l_{CP}}{h}\right)}\left[4+\sqrt{6}\left(\frac{l_{CP}}{h}\right)-9\left(\frac{l_{CP}}{h}\right)^2\right]
$$

$$
+\frac{3\sqrt{6}}{4}\varepsilon_b\left(\frac{E_p}{\Sigma_0}\right)\left(\frac{l_{CP}}{h}\right)^3\ln\left\{1+\frac{\sqrt{6}}{3}\left[\left(\frac{h}{l_{CP}}\right)+\sqrt{\left(\frac{h}{l_{CP}}\right)^2+\sqrt{6}\left(\frac{h}{l_{CP}}\right)}\right]\right\}
$$

$$
+\left[1+\frac{\sqrt{6}}{2}\left(\frac{l_{CP}}{h}\right)\right]\sqrt{1+\sqrt{6}\left(\frac{l_{CP}}{h}\right)}-\frac{3}{2}\left(\frac{l_{CP}}{h}\right)^2
$$

$$
\times\ln\left\{1+\frac{\sqrt{6}}{3}\left[\left(\frac{h}{l_{CP}}\right)+\sqrt{\left(\frac{h}{l_{CP}}\right)^2+\sqrt{6}\left(\frac{h}{l_{CP}}\right)}\right]\right\}. \tag{75}
$$

With the help of values $E_P = 1.03 GPa$ and $\Sigma_0 = 400\,MPa$ for $h = 25, 50, 100$, and $200\,\mu$m given by Shrotriya et al. [22], we use the experimental results (e.g. $h = 25\,\mu$m, $\varepsilon_b = 0.0178$) to calibrate the intrinsic length scales, which results in $l_{FP} = 6.5\,\mu$m and $l_{CP} = 4.8\,\mu$m. Comparisons of the theoretical predictions and the experimental results are shown in Fig. 8. One can see that both the theoretical results have a similar variation trend with the experimental ones. The size effect predicted by C-W gradient theory is a little more obvious than that by CS one.

7 Conclusions

The CS theory and C-W strain gradient one are compared through the model of a micro-cantilever beam bending subject to different loading forms with various material characteristics, such as elastic material, rigid-plastic one. The analytical solutions to deflections have been obtained for both theories. Furthermore, we find the relationship between the intrinsic length scales included in the couple-stress theory proposed by Fleck and Hutchinson [1] and the C-W strain gradient theory suggested by Chen and Wang [2] for an elastic case. The theoretical results predicted by both theories are compared with the experimental ones. It is found that both theories could describe the size effects in cantilever beam bending, and the prediction of the size effect by CS theory is consistent well with the experimental measurements for the thin beam case, while the prediction by C-W theory agrees well with the experimental results for a cantilever beam with a relatively large thickness.

References

1. Fleck, N.A., Hutchinson, J.W.: A phenomenological theory for strain gradient effects in plasticity. J. Mech. Phys. Solids **41**, 1825–1857 (1993)
2. Chen, S.H., Wang, T.C.: A new hardening law for strain gradient plasticity. Acta Mater. **48**, 3997–4005 (2000)
3. Fleck, N.A., Muller, G.M., Ashby, M.F., Hutchinson, J.W.: Strain gradient plasticity theory and experiment. Acta Metallurgica et Materialia **42**, 475–487 (1994)
4. Atkinson, M.: Further analysis of the size effect in indentation hardness tests of some metals. J. Mater. Res. **10**, 2908–2915 (1995)
5. Feng, G., Nix, W.D.: Indentation size effect in MgO. Scr. Mater. **51**, 599–603 (2004)
6. Chen, S.H., Liu, L., Wang, T.C.: Investigation of the mechanical properties of thin films by nano-indentation, considering the effects of thickness and different coating–substrate combinations. Surface and Coatings Technology **191**, 25–32 (2005)
7. Ma, Q., Clarke, D.R.: Size-dependent hardness of silver single-crystals. J. Mater. Res. **10**, 853–863 (1995)
8. McElhaney, K.W., Vlassak, J.J., Nix, W.D.: Determination of indenter tip geometry and indentation contact area for depth-sensing indentation experiments. J. Mater. Res. **13**, 1300–1306 (1998)
9. Nix, W.D.: Mechanical-properties of thin-films. Metallurgical and Materials Transactions A **20**, 2217–2245 (1989)
10. Poole, W.J., Ashby, M.F., Fleck, N.A.: Micro-hardness of annealed and work-hardened copper polycrystals. Scr. Mater. **34**, 559–564 (1996)
11. Saha, R., Nix, W.D.: Effects of the substrate on the determination of thin film mechanical properties by nanoindentation. Acta Mater. **50**, 23–38 (2002)
12. Saha, R., Xue, Z.Y., Huang, Y., Nix, W.D.: Indentation of a soft metal film on a hard substrate: strain gradient hardening effects. J. Mech. Phys. Solids **49**, 1997–2014 (2001)
13. Stelmashenko, N.A., Walls, M.G., Brown, L.M., Milman, Y.V.: Microindentations on W and Mo oriented single crystals: An STM study. Acta Metall. Mater. **41**, 2855–2865 (1993)
14. Swadener, J.G., George, E.P., Pharr, G.M.: The correlation of the indentation size effect measured with indenters of various shapes. J. Mech. Phys. Solids **50**, 681–694 (2002)
15. Yang, J., Cady, C., Hu, M.S., Zok, F., Mehrabian, R., Evans, A.G.: Effects of damage of the flow strength and ductility of a ductile Al-alloy reinforced with SiC particulates. Acta Metall. Mater. **38**, 2613–2619 (1990)
16. Li, X.D., Bhushan, B., Takashima, K., Baek, C.W., Kim, Y.K.: Mechanical characterization of micro/nanoscale structures for MEMS/NEMS applications using nanoindentation techniques. Ultramicroscopy **97**, 481–494 (2003)
17. Pei, J.H., Tian, F., Thundat, T.: Glucose biosensor based on the microcantilever. Anal. Chem. **76**, 292–297 (2004)
18. Pereira, R.D.: Atomic force microscopy as a novel pharmacological tool. Biochem. Pharmacol. **62**, 975–983 (2001)
19. Ehrler, B., Hou, X.D., Zhu, T.T., Png, K.M.Y., Walker, C.J., Bushby, A.J., Dunstan, D.J.: Grain size and sample size interact to determine strength in a soft metal. Phil. Mag. **88**, 3043–3050 (2008)
20. Haque, M.A., Saif, M.T.A.: Strain gradient effect in nanoscale thin films. Acta Mater. **51**, 3053–3061 (2003)
21. Lam, D.C.C., Yang, F., Chong, A.C.M., Wang, J., Tong, P.: Experiments and theory in strain gradient elasticity. J. Mech. Phys. Solids **51**, 1477–1508 (2003)
22. Shrotriya, P., Allameh, S.M., Lou, J., Buchheit, T., Soboyejo, W.O.: On the measurement of the plasticity length scale parameter in LIGA nickel foils. Mech. Mater. **35**, 233–243 (2003)
23. Stolken, J.S., Evans, A.G.: A microbend test method for measuring the plasticity length scale. Acta Mater. **46**, 5109–5115 (1998)
24. Hall, E.O.: Variation of hardness of metals with grain size. Nature **173**, 948–949 (1954)
25. Weertman, J.R.: Hall-petch strengthening in nanocrystalline metals. Mater. Sci. Eng. A Struct. Mater. Prop. Microstruct. Process. **166**, 161–167 (1993)
26. Elssner, G., Korn, D., Ruhle, M.: The influence of interface impurities on fracture energy of UHV diffusion-bonded metal-ceramic bicrystals. Scripta Metall. Mater. **31**, 1037–1042 (1994)
27. Mindlin, R.D.: Micro-structure in linear elasticity. Arch. Rat. Mech. Anal. **16**, 51–78 (1964)
28. Mindlin, R.D.: Second gradient of strain and surface tension in linear elasticity. Int. J. Solids Struct. **1**, 417–438 (1965)
29. Fleck, N.A., Hutchinson, J.W.: Strain gradient plasticity. In: Hutchinson, J.W., Wu, T.Y. (eds.) Advances in Applied Mechanics, vol. 33, pp. 295–361. Academic Press, New York (1997)
30. Fleck, N.A., Hutchinson, J.W.: A reformulation of strain gradient plasticity. J. Mech. Phys. Solids **49**, 2245–2271 (2001)
31. Fleck, N.A., Willis, J.R.: A mathematical basis for strain-gradient plasticity theory. Part II: tensorial plastic multiplier. J. Mech. Phys. Solids **57**, 1045–1057 (2009)
32. Gao, H., Huang, Y., Nix, W.D.: Modeling plasticity at the micrometer scale. Naturwissenschaften **86**, 507–515 (1999)
33. Gao, H., Huang, Y., Nix, W.D., Hutchinson, J.W.: Mechanism-based strain gradient plasticity-I. Theory. J. Mech. Phys. Solids **47**, 1239–1263 (1999)
34. Gurtin, M.E.: On the plasticity of single crystals: free energy, microforces, plastic-strain gradients. J. Mech. Phys. Solids **48**, 989–1036 (2000)
35. Gurtin, M.E.: A gradient theory of single-crystal viscoplasticity that accounts for geometrically necessary dislocations. J. Mech. Phys. Solids **50**, 5–32 (2002)
36. Huang, Y., Gao, H., Nix, W.D., Hutchinson, J.W.: Mechanism-based strain gradient plasticity-II. Analysis. J. Mech. Phys. Solids **48**, 99–128 (2000)
37. Huang, Y., Xue, Z., Gao, H., Nix, W.D., Xia, Z.C.: A study of microindentation hardness tests by mechanism-based strain gradient plasticity. J. Mater. Res. **15**, 1786–1796 (2000)
38. Hwang, K.C., Jiang, H., Huang, Y., Gao, H.: Finite deformation analysis of mechanism-based strain gradient plasticity: torsion and crack tip field. Int. J. Plast. **19**, 235–251 (2003)
39. Hwang, K.C., Jiang, H., Huang, Y., Gao, H., Hu, N.: A finite deformation theory of strain gradient plasticity. J. Mech. Phys. Solids **50**, 81–99 (2002)

40. Yang, F., Chong, A.C.M., Lam, D.C.C., Tong, P.: Couple stress based strain gradient theory for elasticity. Int. J. Solids Struct. **39**, 2731–2743 (2002)
41. Yi, D.K., Wang, T.C., Chen, S.H.: New strain gradient theory and analysis. Acta Mech. Solida Sin. **22**, 45–52 (2009)
42. Acharya, A., Beaudoin, A.J.: Grain-size effect in viscoplastic polycrystals at moderate strains. J. Mech. Phys. Solids **48**, 2213–2230 (2000)
43. Bassani, J.L.: Incompatibility and a simple gradient theory of plasticity. J. Mech. Phys. Solids **49**, 1983–1996 (2001)
44. Evers, L.P., Parks, D.M., Brekelmans, W.A.M., Geers, M.G.D.: Crystal plasticity model with enhanced hardening by geometrically necessary dislocation accumulation. J. Mech. Phys. Solids **50**, 2403–2424 (2002)
45. Huang, Y., Qu, S., Hwang, K.C., Li, M., Gao, H.: A conventional theory of mechanism-based strain gradient plasticity. Int. J. Plast. **20**, 753–782 (2004)
46. Peerlings, R.H.J., deBorst, R., Brekelmans, W.A.M., deVree, J.H.P.: Gradient enhanced damage for quasi-brittle materials. Int. J. Numer. Methods Eng. **39**, 3391–3403 (1996)
47. Voyiadjis, G.Z., Deliktas, B., Aifantis, E.C.: Multiscale analysis of multiple damage mechanisms coupled with inelastic behavior of composite materials. J. Eng. Mech. ASCE **127**, 636–645 (2001)
48. Voyiadjis, G.Z., Dorgan, R.J.: Gradient formulation in coupled damage-plasticity. Arch. Mech. **53**, 565–597 (2001)
49. Aifantis, E.C., Oka, F., Yashima, A., Adachi, T.: Instability of gradient dependent elasto-viscoplasticity for clay. Int. J. Numer. Anal. Methods Geomech. **23**, 973–994 (1999)
50. Gurtin, M.E.: On a framework for small-deformation viscoplasticity: free energy, microforces, strain gradients. Int. J. Plast. **19**, 47–90 (2003)
51. Voyiadjis, G.Z., Abu Al-Rub, R.K., Palazotto, A.N.: Non-local coupling of viscoplasticity and anisotropic viscodamage for impact problems using the gradient theory. Arch. Mech. **55**, 39–89 (2003)
52. Wang, W.M., Askes, H., Sluys, L.J.: Gradient viscoplastic modelling of material instabilities in metals. Metal. Mater. Int. **4**, 537–542 (1998)
53. Chen, S.H., Wang, T.C.: A new deformation theory with strain gradient effects. Int. J. Plast. **18**, 971–995 (2002)
54. Chen, S.H, Wang, T.C.: Strain gradient theory with couple stress for crystalline solids. Eur. J. Mech. A Solids **20**, 739–756 (2001)
55. Gao, H.J., Huang, Y.G.: Taylor-based nonlocal theory of plasticity. Int. J. Solids Struct. **38**, 2615–2637 (2001)
56. Chen, S.H., Liu, L., Wang, T.C.: Size dependent nanoindentation of a soft film on a hard substrate. Acta Mater. **52**, 1089–1095 (2004)
57. Nix, W.D., Gao, H.J.: Indentation size effects in crystalline materials: a law for strain gradient plasticity. J. Mech. Phys. Solids **46**, 411–425 (1998)
58. Wei, Y., Hutchinson, J.W.: Hardness trends in micro scale indentation. J. Mech. Phys. Solids **51**, 2037–2056 (2003)
59. Xue, Z., Huang, Y., Hwang, K.C., Li, M.: The influence of indenter tip radius on the micro-indentation hardness. J. Eng. Mater. Tech. **124**, 371–379 (2002)
60. Chen, S.H., Wang, T.C.: Size effects in the particle-reinforced metal-matrix composites. Acta Mech. **157**, 113–127 (2002)
61. Shu, J.Y., Fleck, N.A.: Strain gradient crystal plasticity: size-dependent deformation of bicrystals. J. Mech. Phys. Solids **47**, 297–324 (1999)
62. Wei, Y.: Particulate size effects in the particle-reinforced metal-matrix composites. Acta Mech. Sin. **17**, 45–58 (2001)
63. Liu, X., Hu, G.: A continuum micromechanical theory of overall plasticity for particulate composites including particle size effect. Int. J. Plast. **21**, 777–799 (2005)
64. Voyiadjis, G.Z., Abu Al-Rub, R.K.: Gradient plasticity theory with a variable length scale parameter. Int. J. Solids Struct. **42**, 3998–4029 (2005)
65. Hu, G.K., Liu, X.N., Lu, T.J.: A variational method for non-linear micropolar composites. Mech. Mater. **37**, 407–425 (2005)
66. Wang, W., Huang, Y., Hsia, K.J., Hu, K.X., Chandra, A.: A study of microbend test by strain gradient plasticity. Int. J. Plast. **19**, 365–382 (2003)
67. McFarland, A.W., Colton, J.S.: Role of material microstructure in plate stiffness with relevance to microcantilever sensors. J. Micromech. Microeng. **15**, 1060–1067 (2005)
68. Park, S.K., Gao, X.L.: Bernoulli-Euler beam model based on a modified couple stress theory. J. Micromech. Microeng. **16**, 2355–2359 (2006)
69. Ma, H.M., Gao, X.L., Reddy, J.N.: A microstructure-dependent Timoshenko beam model based on a modified couple stress theory. J. Mech. Phys. Solids **56**, 3379–3391 (2008)
70. Challamel, N., Wang, C.M.: The small length scale effect for a non-local cantilever beam: a paradox solved. Nanotechnology **19**, 345703 (2008)
71. Giannakopoulos, A.E., Stamoulis, K.: Structural analysis of gradient elastic components. Int. J. Solids Struct. **44**, 3440–3451 (2007)
72. Ji, B., Chen, W.J., Zhao, J.: Measurement of length-scale and solution of cantilever beam in couple stress elasto-plasticity. Acta Mech. Sin. **25**, 381–387 (2009)
73. Shi, Z.F., Huang, B., Tan, H., Huang, Y., Zhang, T.Y., Wu, P.D., Hwang, K.C., Gao, H.: Determination of the microscale stress-strain curve and strain gradient effect from the micro-bend of ultra-thin beams. Int. J. Plast. **24**, 1606–1624 (2008)
74. Mindlin, R.D., Tiersten, H.F.: Effects of couple-stress in linear elasticity. Arch. Rat. Mech. Anal. **11**, 415–448 (1963)
75. Toupin, R.A.: Elastic materials with couple-stresses. Arch. Rat. Mech. Anal. **11**, 385–414 (1963)
76. Acharya, A., Bassani, J.L. : On nonlocal flow theories that preserve the classical structure of incremental boundary value problems. In: Pineau, A., Zaoui, A. (eds.) IUTAM Symposium on Micromechanics of Plasticity and Damage of Multiphase Materials, pp. 3–9. Kluwer Academic Publishers, Dordrecht (1996)
77. Acharya, A., Bassani, J.L.: Lattice incompatibility and a gradient theory of crystal plasticity. J. Mech. Phys. Solids **48**, 1565–1595 (2000)
78. Acharya, A., Tang, H., Saigal, S., Bassani, J.L.: On boundary conditions and plastic strain-gradient discontinuity in lower-order gradient plasticity. J. Mech. Phys. Solids **52**, 1793–1826 (2004)

79. Volokh, K.Yu., Hutchinson, J.W.: Are lower-order gradient theories of plasticity really lower order? J. Appl. Mech. **69**, 862–864 (2002)
80. Niordson, C.F., Hutchinson, J.W.: On lower-order strain gradient plasticity theories. Eur. J. Mech. A Solids **22**, 771–778 (2003)
81. Gurtin, M.E., Anand, L.: Thermodynamics applied to gradient theories involving the accumulated plastic strain: the theories of Aifantis and Fleck and Hutchinson and their generalization. J. Mech. Phys. Solids **57**, 405–421 (2009)
82. Aifantis, E.C: The physics of plastic deformation. Int. J. Plast. **3**, 259–280 (1987)
83. Kuroda, M. Tvergaard, V.: An alternative treatment of phenomenological higher-order strain-gradient plasticity theory. Int. J. Plast. **26**, 507–515 (2010)
84. Mühlhaus, H.B., Aifantis, E.C.: A variational principle for gradient plasticity. Int. J. Solids Struct. **28**, 845–857 (1991)
85. Abu Al-Rub, R.K., Voyiadjis, G.Z., Bammann, D.J.: A thermodynamic based higher-order gradient theory for size dependent plasticity. Int. J. Solids Struct. **44**, 2888–2923 (2007)
86. Reddy, J.N.: Nonlocal theories for bending, buckling and vibration of beams. Int. J. Eng. Sci. **45**, 288–307 (2007)
87. Shames, I.H., Dym, C.L.: Energy and finite element methods in structural mechanics. Hemisphere Pub. Corp., New York (1985)
88. Zhu, H.X.: Large deformation pure bending of an elastic plastic power-law-hardening wide plate: Analysis and application. Int. J. Mech. Sci. **49**, 500–514 (2007)